Limit states of reinforced concrete bridge piers confined with carbon fiber reinforced polymer (CFRP)

Michael Jean, Charles St-Martin, Nathalie Roy, Patrice Rivard, Zabihallah Moradian, Eduardo Carvalho Jr & Jean Proulx
University of Sherbrooke, Canada

SUMMARY:

Over the past 20 years, several earthquakes (e.g. Northridge 1994 to Chile 2010) caused severe damage to a large number of bridges. Lessons learned from these events led to the development of innovative retrofitting techniques in order to improve the seismic behavior of potentially deficient structures. One of these techniques—wrapping RC columns with carbon-fiber-reinforced polymers (CFRPs)—is now known to improve the seismic response of such critical elements. Confining RC columns with CFRPs increases their ductility and energy dissipation during an earthquake. This paper presents new limit states for such columns, based on an experimental program during which four columns were tested. Each column is 2 m height and 300 mm in diameter. The yielding of the longitudinal and transverse reinforcement, cracks in concrete and the rupture of the FRP were monitored in real time with a non-destructive method called ultrasonic pulse velocity (UPV). A numerical model was developed with OpenSees. Engineering damage parameters (EDP) were studied and new limit states are proposed for the bridge columns tested in this project (under an axial load ratio of $0.1A_g f'_c$).

Keywords: RC Bridge Columns, Ductility, CFRPs, Performance-based design, limit states

1. INTRODUCTION

Important earthquakes can inflict significant to major damages to bridge structures, and in some cases even cause collapse. Some recent earthquakes that resulted in such damage happened in Northridge (1994), Loma Prieta (1989) and Chile (2010). The Northridge (1994) event itself caused damages on 1364 bridges and all of them needed reinforcement or repair before reopening. In the case of RC bridge columns, the deterioration from cyclic loading is mostly concentrated in the plastic hinge region at the base. Bar slip, longitudinal reinforcement buckling, spalling of concrete and loss of anchorage are the most frequent damages observed. For a standard reinforced concrete pile, the damages start with the cracking of concrete cover, and then the longitudinal and transverse reinforcement starts yielding. Afterwards, the concrete core crushes and spalls, which in turn causes buckling or breaking of the longitudinal reinforcement. This sequence of damages constitutes the limit states for RC bridge columns. Confinement of the colums can change the sequence of the damage process. This is why this approach, for example using carbon fibre reinforced polymers (CFRP), is one of the most efficient methods to improve the seismic performance of RC bridge columns. This paper proposes new limit states that describe the performance of RC bridge columns confined with FRP. Results of an experimental program and a numerical study are presented. The limit states are corroborated with results of non-destructive tests performed on RC columns confined with CFRP and submitted to cyclic tests.

2. LIMIT STATES

In addition to protecting human lives, the use of a performance-based evaluation and retrofit approach is meant to reduce damage and the inherent costs of repair due to moderate earthquakes. In its 2000 and 2006 editions, the Canadian Highway Bridge Design Code (CHBDC 2000 and 2006) has specified some performance objectives, criteria and corresponding seismic hazard. The three objectives relate to the functionality of the bridge, ranging from "fully operational" to "life safety". It should be noted that the actual performance criteria, defined in terms of level of service and corresponding damage, are essentially qualitative. It is essential to quantify the damage for each level in order to associate the structure response to its performance. The capacities of the bridge components such as columns are defined in terms of limit states. Traditionally, these limit states for bridge components have been defined by qualitative damage states such as "slight", "moderate", "extensive" and "complete". With the definition of qualitative damage states, quantitative limit states must now be explicited. Figure 2.1 shows damage states for both unconfined and CFRPs-confined RC columns.

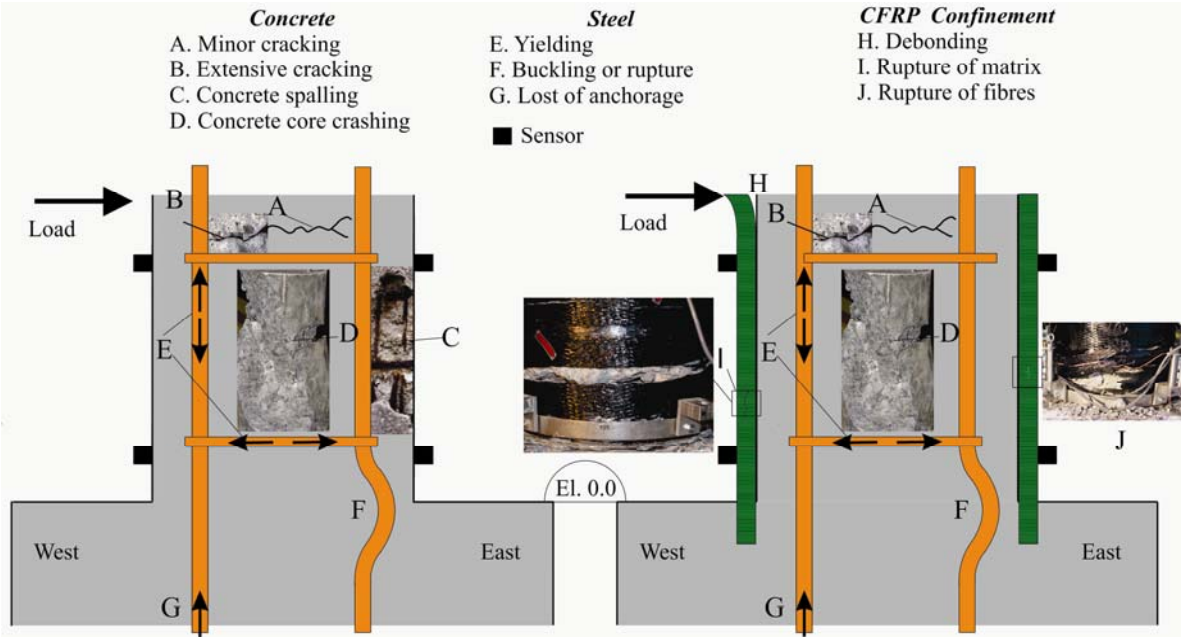

Figure 2.1. (a) RC column damages and (b) RC column confined with CFRPs damages

2.1. Damage progression in unconfined RC columns and RC columns confined with CFRP

The first damage to occur in columns is the cracking of the concrete cover, which causes a slight decrease of the stiffness of the element. Depending on the width of the cracks, epoxy injections can be necessary to repair the column (Lehman et al. 2004). The next step is yielding of the longitudinal reinforcement, followed by extensive concrete cracking concrete. Axial strains in the cover increase until it begins to spall. With this level of damage, epoxy injections are not sufficient and the replacement of the concrete cover would be necessary to repair the column. With the loss of concrete cover, the strains in longitudinal reinforcement and concrete core will increase. The concrete core expansion will induce more strain in the transverse reinforcement. Passive confinement, provided by transverse reinforcement, restricts this expansion of the concrete core, depending on its stiffness. The combination of strains and transversal stresses caused by the core expansion amplify the buckling hazard of the longitudinal bars. If the spacing of the transverse reinforcement is too wide, the confinement pressure is insufficient to prevent buckling or core crushing. Even with smaller spacing and increased confinement, the longitudinal bars can reach their

ultimate strain. In both cases, the column could not be repaired and would have to be replaced.
The additional external confinement provided by CFRPs allows the concrete to sustain more axial load (Samaan et al. 1998). CFRP is a passive confinement that has an effect only when the concrete expands. The confinement pressure is constant according to the elastic behaviour of the material. In fact, the use of CFRP restrains the concrete expansion. Thus, the damage sequence now starts with yielding of the longitudinal and transverse reinforcement. It is followed by the rupture of the CFRP matrix. Rupture of the CFRP fibers, and then buckling or rupture of the longitudinal reinforcement (fig. 2.2) will occur at ultimate loading. Spalling of the concrete cover is no longer a limit state. Moreover, concrete cracking, yielding of the transverse reinforcement and failure of the longitudinal reinforcement are all delayed and will occur at larger displacements and ductility ratios.

2.2. Existing limit states for RC columns

In performance-based design, it is common to use the following engineering damage parameters (EDP): sectional (μ_ϕ) or displacement ductility (μ_Δ), drift ratio (δ) and concrete strain (ε_{cu}) to quantify the damage levels expected under a given seismic demand. The ductility is very useful since it provides information on the plastic hinge region which suffers most of the damages in a RC column (Legeron 1998). Mainly used for buildings, the drift ratio is also common and is related to the length of element. Table 2.1 presents different limits states according to different performance level available in the literature. Displacement ductility, μ_Δ, (Priestley et al. 1996), drift, δ, (Ghobarah 2001) and concrete strain, $\varepsilon_{cu,}$ (Lehman et al. 2004) are presented in this table.

Table 2.1 Limit states according to different damage levels

Damage Level	EDP values for RC piers		
	Ductility (μ_Δ)	Drift (δ)	Concrete strain (ε_{cu})
1 – No Damage	2	<0.2%	
2 – Medium Damage	3	<0.4%	0.0039 to 0.011
3 – Important Damage	6	<2.5%	0.010 to 0.029

These performance levels and EDP values are defined for conventional reinforced concrete. The presence of CFRPs greatly increases the ductility that the section can reach at its ultimate state. Boucher-Trudeau (2006) tested four CFRP-confined RC columns with L/D ratio = 6.7, two different axial load ratio ($0.10A_gf'_c$, $0.35A_gf'_c$) and two different stirrups pitch (75mm, 150mm) under cyclic loading. The specimens reached drift ratios ranging from 8% ($0.35A_gf'_c$) to 14% ($0.10A_gf'_c$), and displacement ductilities between 6 ($0.35A_gf'_c$) and 8 ($0.10A_gf'_c$) at failure. According to these results, the limit states given in table 2.1 are not accurate for RC columns confined with CFRPs.

3. EXPERIMENTAL PROGRAM

Cyclic tests were carried out on a series of four large-scale circular columns with properties defined to be representative of typical piers belonging to short-span bridges. The 2-m high columns have a 300-mm diameter and are embedded in a massive foundation that was anchored to a strong floor for the tests. A constant axial force (corresponding to $0.10A_gf'_c$ and $0.25A_gf'_c$) was applied to the columns by means of two hydraulic actuators.. Prescribed displacement histories were imposed on the column by means of a 500-kN double-acting displacement-controlled servo-hydraulic actuator reacting on a large-capacity vertical reaction wall. The purpose of the first cycle was to induce cracking in the column and to identify its initial elastic characteristics. In this cycle, the maximum horizontal load was set to reach 75% of the expected yield load. During the second cycle, the yield load was attained and the corresponding yield displacement was identified. Each subsequent cycle was repeated twice with a maximum displacement equal to 1.5, 2, 3, … times the measured yield displacement up to failure. Table 4.1 provides the 28-day

concrete strength of each column. The CFRP-confinement corresponds to one layer (1.016 mm) of SikaWrap C103 and Sikadur 300 resin (ε_{frp} = 0.09767). The longitudinal and transversal reinforcement consisted of six 20M rebars (f_y = 431MPa) and 10M stirrups (f_y = 503MPa).

Table 3.1. Specimens description

Parameters	Columns			
	S75P10C1	S75P35C1	S150P10C1	S150P35C1
Concrete strength (f'_c) (MPa)	34	36	36	37
Axial load (P) (kN)	230	663	222	636
Steel pitch (s) (mm)	75	75	150	150

4. NUMERICAL MODELLING

Numerical analyses were carried out for the four CFRP-confined columns. A distributed plasticity approach was selected as the analysis method for this project. . With this method, plasticity can spread along the column. An efficiency factor of 80% was chosen for the ultimate FRP strain. This value can vary from 70% to 80% according Eid and Paultre, 2008.

The specimens were modeled using multifiber analysis with the OpenSees open-source platform (Mazzoni et al., 2006). Analysis efficiency depends on the number of fibers (Berry and Eberhard, 2008). The column section was discretized into 200 fibers, each with its own stress–strain behavior that represents material behavior. The Eid and Paultre model (2008) was used for the confined concrete with the Concrete01 option in OpenSees. The concrete cover, confined with CFRP alone, and the concrete core, confined with steel and CFRP, were implemented using two different materials. For the steel bar, the Steel02 option was used and the model was calibrated with the results from tension tests on the steel bars carried out by Carvalho (2012). A strain hardening ratio of 0.02 was selected. According to Calabrese, 2010, this value is accurate in order to prevent strain localization problems.

The nonlinear Beam Column option selected for the model uses a flexibility formulation with interpolation functions for internal forces. This method is more efficient than the rigidity formulation (Neuenhofer and Filippou, 1997). The interpolation can be cubic between the Gauss integration point, whereas the stiffness method uses linear interpolation.

4.1 Confinement modeling

There are many available confinement models for FRPs (De Lorenzis and Tepfers, 2003), but only a few take into account the combined effects of confinement from both the transverse steel reinforcement and the CFRPs (Eid and Paultre, 2008; Gallardo-Zafra and Kawashima, 2009; Pellegrino and Modena, 2010). Under axial load, concrete expands laterally in proportion to its Poisson's ratio. The value of this ratio will increase with damage and can range from 0.15 to 0.45 (Eid and Paultre, 2008). Confinement with transverse steel reinforcement will help to partly delay this phenomenon. Nevertheless, the elastic–perfectly plastic behavior of steel will cause some instability in the volumetric deformations when the transverse reinforcement reaches plastic behavior (Samaan et al. 1998). The lateral pressure on the concrete core from the transverse steel will remain constant after this point (Teng and Lam, 2004). On the other hand, CFRPs have a purely elastic behavior. It restrains the concrete section in a more stable way throughout loading (Samaan et al., 1998) and its lateral pressure increases linearly until failure (Teng and Lam., 2004). Figure 4.1 shows the behavior of a 300-mm circular concrete section alone, the same section confined with transverse steel reinforcement with 75-mm pitch and, lastly, confined with both steel and CFRP. Most RC-bridge columns contain the minimum transverse steel reinforcement prescribed in design

codes. It is therefore important to use a confinement model that takes into account the effects of confinement from both steel and CFRP in order to accurately predict the behavior of RC columns under cyclic loading. In this research project, the Eid and Paultre model (2008) was selected to represent the behavior of the RC columns analyzed.

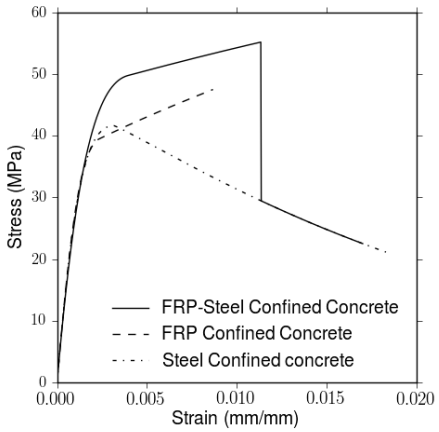

Fig. 4.1 Concrete stress-strain curves

5. RESULTS

5.1 Experimental results

The load-displacement curves of each column are shown in Figures 5.1 and 5.2. The first event observed is the yielding of the longitudinal bars. During the first cycles, some cracks appeared in the CFRP matrix in the direction parallel to the fibres at a height ranging between 80mm and 240mm above the foundation for each column. During the tests, some large cracks with widths of up to 5mm have been observed. CFRP failure occurred at ductility values ranging from 5 (for specimen S150P35C1 in Table 3.1) to 11 (S75P10C1) depending on the axial load ratio. Only the S150P10C1 specimen did not reached this level because the damage occurred mainly in the foundation. Diagonal cracks and concrete spalling were observed for this column indicating foundation rotation. With the loss of CFRP confinement, the concrete then crushed. Following this, at least one longitudinal bar failed for each column in the next cycles.

5.2 Numerical results

Figures 5.1 and 5.2 present the numerical results for the 4 columns that were tested. The observed hysteretic behavior is accurately represented by the analytical models. The unloading branch of the loops and the pinching are effectively modelled. The CFRP ruptures are well predicted for three columns. In the case of specimen S150P10C1 (fig. 5.2. a), the model is not quite as representative, as the foundation of this column suffered extensive damage. The ductility values corresponding to yielding of stirrups range from 2 to 5.

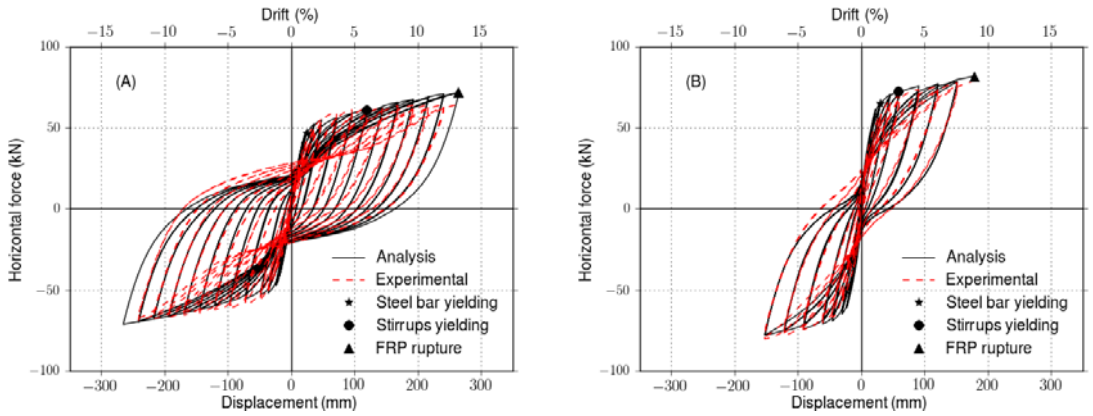

Figure 5.1. Experimental and analysis response of (a) S75P10C1 and (b) S75P35C1

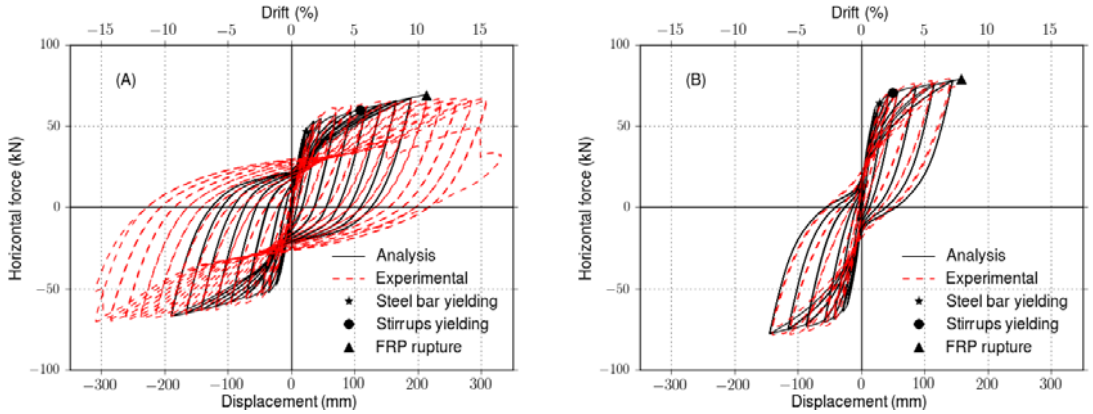

Figure 5.2. Experimental and analysis response of (a) S150P10C1 and (b) S150P35C1

The work index (I_w) (eq. 5.1) was calculated to quantify the relative damage at each cycle.

$$I_w = \sum_{i=1}^{n} \frac{H_i \Delta_i}{H_{max} \Delta_{yi}} \tag{5.1}$$

The relative damage index (I_{wi}/I_w) and the maximum strain in concrete according to ductility values are plotted in fig. 5.3. The results shown in this figure are used to determine the new limit states in the next section.

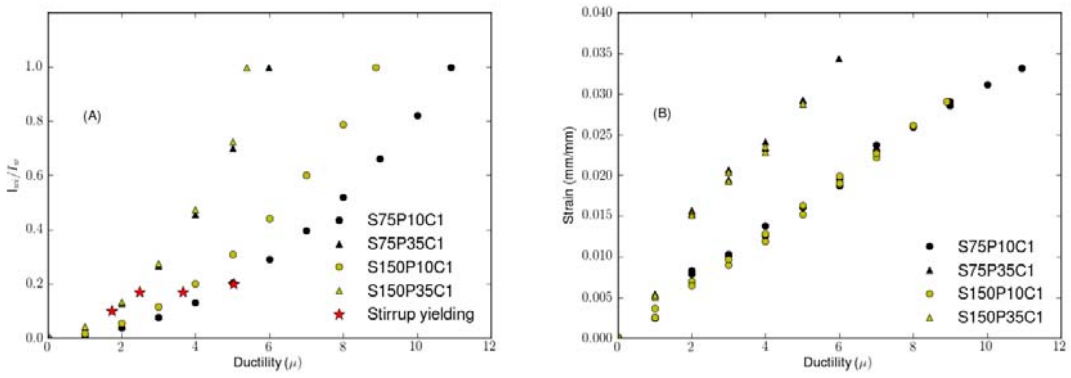

Figure 5.3. Damage (I_w) vs ductility (a) and concrete strain vs ductility (b)

5.3 Ultrasonic pulse velocity results

The CFRP confinement makes it difficult to monitor and predict the damage after events like earthquakes. The condition of the concrete can be assessed using ultrasonic pulse velocity (UPV) measurements. This nondestructive method was used in this study to determine the state of damage in the columns. Among the evaluation methods frequently used for concrete structures, UPV is a simple and quick method. UPV consists of measuring the propagation time of compression waves (P waves) between two sensors, also called time-of-flight (TOF), a value that can be converted into velocity. This velocity mainly depends on the elastic properties of the concrete, thus being related to the rate of damage in the column. A low velocity is indicative of a poor concrete, i.e. high damage. Table 5.1 shows a quantification of the damage and mechanical properties of concrete as a function of the velocity. Velocity measurements were taken at six different locations on the columns in the east/west direction (Fig. 5.4). The measured points were selected in order to cover the expected damaged zone (elevation 0, 100, 200, 300, 400 and 500mm). The velocities were measured before the test, after the $1\Delta_y$ cycles, the $2\Delta_y$ cycles, and so on until the end of the test.

Table 5.1 Concrete velocity according to damage (Bullock 1959)

Cote	Quality of concrete	V (m/s)
(1)	Excellent	> 4500
(2)	Good	3500 - 4500
(3)	Doubtful	3000 - 3500
(4)	Poor	2000 - 3000
(5)	Very poor	< 2000

The five levels of damage according to Bullock (1959) are represented by shaded areas in Fig 5.4. The results were compiled until the end of the test. When measurements were not possible, the value 0 was assigned. Kim (1998) has developed a damage index, ω, to determine the state of damage in concrete (Eqn 5.2). V_p is the initial velocity and V'_p is the velocity taken during the test. The damage indices are shown in fig. 5.5. The results shown in this figure are used to confirm the new limit states in the next section.

$$\omega = 1 - \left(\frac{V_{t_p}}{V_p}\right)^2 \tag{5.2}$$

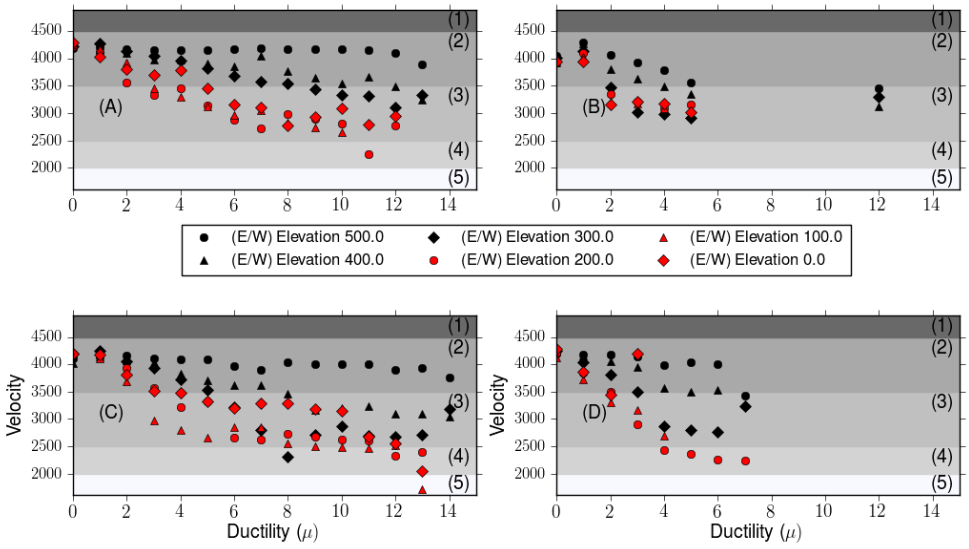

Fig 5.4. Velocity vs ductility for (a) S75P10C1 (b) S150P10C1 (c) S75P35C1 (d) S150P35C1

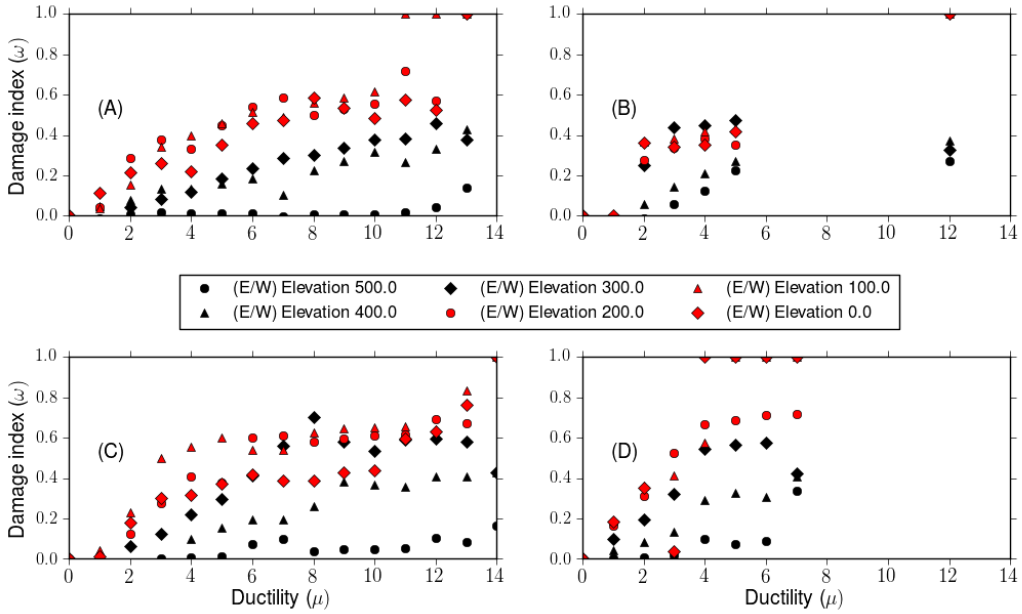

Fig 5.5. Damage index for (a) S75P10C1 (b) S150P10C1 (c) S75P35C1 (d) S150P35C1

6. DISCUSSION

As shown in figure 5.3a, the columns reached ductility values higher than those given for limit states of unconfined RC column in Table 2.1. In this Table, a ductility of 3 was associated to medium damage, which represents cover crack and spalling. For this state, rehabilitation interventions are necessary to maintain serviceability. The columns confined with CFRP reached a maximum relative damage index (I_{wi}/I_w) of 30% for this ductility value. At this level, serviceability is maintained and no intervention is required. Moreover, the stirrup yielding did not occur for columns with an axial load of $0.1A_gf'_c$ for this ductility value, as observed on fig 5.1a and 5.2a.

Confined columns S75P10C1 and S150P10C1 ($0.1A_gf'_c$) reached ductility values of at least 8 before CFRP rupture (value of I_{wi}/I_w =1 on fig. 5.3a). The recommended ductility value for severe damage of 6 given in Table 2.1, and recommended by Priestley et al. 1996, was defined for bridge piers which are commonly subjected to axial loads corresponding to $0.1A_gf'_c$. Therefore, this value is not accurate for RC bridge columns confined with CFRP.

The concrete strain recommended for the limit states of unconfined RC columns can also be compared with the results from nonlinear analysis for RC columns confined with CFRP. The concrete strain corresponding to serviceability levels varies from 0.0039 to 0.011. For the CFRP-confined RC columns (fig. 5.3b), this strain represents a maximum value of less than 20% of the ultimate work index (I_w) for bridge columns ($0.1A_gf'_c$). No damage has been observed during the test at this stage. For important damages, a value of 0.02 was proposed for RC columns. According to results, the concrete ultimate strain corresponding at CFRP rupture is higher than that and is closer to 0.035.

Using the UPV measurements (fig. 5.4) it is possible to predict the failure of FRP using measurements taken at elevations from 0 to 400 mm. In fact, when the damage index becomes higher than 0.5 and when the velocity drops below 3000 m/s, the rupture of FRP occurs at the next Δ_y increment. Damage in

concrete appears to vary linearly until the rupture of the FRP. The UPV results from 0 to 400 mm show a correlation with the analysis model versus the damage limit states. As shown in Figure 5.4 and 5.5,it can be noted that for specimen S150P35C1 at a ductility of 3, the damage variable is approximately 0.4 and the concrete damage is moderate (UPV velocity ≈ 3300 m/ s). Moreover, for columns axially loaded to 10%, the damage variable is close to 0.5 and there is moderate damage in concrete (≈3300 m/ s) at a ductility of 6.

Based on all these experimental results and observations, new (quantitative) limit states are proposed for the bridge columns tested in this project (under an axial load ratio of $0.1A_gf'_c$). They are summarized in Table 6.1.

Table 6.1 Limit states for RC bridge column confined with CFRP ($P=0.1A_gf'_c$)

Damage level	Recommended values in the literature and corresponding damage state				Proposed values and corresponding damage state for the tested columns			
	Damage	ε_c	μ	I_{wi}/I_w	Damage	ε_c	μ	I_{wi}/I_w
Moderate	Spalling of concrete	0.004 – 0.011	3	0.15	Yielding of transversal steel	0.02	4-5	0.40
Severe	Concrete core crushing	0.02	6	0.40	Failure of CFRP	0.035	8	1.00

7. CONCLUSIONS

For standard reinforced concrete columns, damages begin with the cracking of the concrete cover, and then the longitudinal and transverse reinforcement starts yielding. At this moment, the concrete core crushes and spalls, which in turn causes buckling or failure of the longitudinal reinforcement. This sequence of damage represents the limit states for a normal RC bridge column. Adding external CFRP confinement changes this sequence. Yielding of the longitudinal and transverse reinforcement becomes the first step, followed by the CFRP matrix rupture. Buckling or failure of the longitudinal reinforcement then occurs. Spalling of the concrete cover is no longer a limit state. Moreover, cracks in concrete, yielding of the transverse reinforcement and failure of the longitudinal reinforcement are all delayed and will occur at larger displacements and ductility ratios. Based on numerical analysis results and UPV measurements obtained during the cyclic tests, it was observed that limit states recommended for standard RC columns do not apply for RC columns confined with CFRP under an axial load of $0.1A_gf'_c$, which corresponds to typical values for bridges. New values of limit states for moderate and severe damage levels were proposed, based on experimental results, finite-element analysis and UPV measurements.

ACKNOWLEDGMENTS

The authors would like to acknowledge the financial support of the Natural Sciences and Engineering Research Council of Canada (NSERC) and Sika-Canada.

REFERENCES

Boucher-Trudeau, M. (2010). Behavior of cicular RC concrete columns confined with CFRPs under flexure and axial load. *In French.*
Masters Thesis, University of Sherbrooke.

Bullock, R. E., Whitehurst, E. A. (1959). Effect of certain variables on Pulse Velocities through Concrete. *Highw, Res. Board Bull*., **206**, 37.

Calabrese, A., Almeida, J. P. and Pinho, R. (2010). Numerical issues in distributed inelasticity modeling of RC frame for seismic analysis. *Journal of Earthquake Engineering*. **Vol 14**, 38-68.

CAN/CSA-S6-06 (2006).Canadian Highway Bridge Design Code (CHBDC) (CAN/CSA-S6-06). Canadian Standards Association (CSA), Toronto, Ontario, Canada.

Carvalho, E. (2012). Evaluation of the plastic hinge length in concrete columns confined with CFRPs. *In French.* . Masters Thesis, University of Sherbrooke.

De Lorenzis, L., and Tepfers, R. (2003). Comparative study of models on confinement of Concrete Cylinders with fiber- reinforced polymer composites. *Journal of Composites for Construction.* **7: 3**, 219-237.

Eid, R. and Paultre, P. (2008). Analytical model for FRP-confined circular reinforced concrete columns. Journal *of Composites for Construction, ASCE,* **12:56**, 541-552.

Gallardo-Zafra, R. et Kawashima, K. (2009). Analysis of carbon fiber sheet-retrofitted RC bridge columns under lateral cyclic loading. *Journal of Earthquake Engineering*. **13:2**,129-154.

Ghobarah, Ahamed (2001). Performance-based design in earthquake engineering: state of development. *Engineering Structures*. **Vol 23**, 878-884.

Gu, D.-S., Wu, Y.-F., Wu, G. and Shen Wu, Z. (2011). Plastic hinge analysis of FRP confined circular concrete columns. *Construction and Building Materials*, at press.

Kim, D.S. and McCarter, M. K. (1998). Quantitative assessment of extrinsic damage in rock materials. *Rock Mechanics and Rock Engineering*, **Vol 31**, 43-62.

Légeron, F. (1998). Comportement sismique des structures en béton ordinaire et en béton à haute performance armé. Ph. D. thesis, University of Sherbrooke and École Nationale des Ponts et Chaussées.

Lehman, D., Moehle, J., Mahin, S., Calderone, A. And Henry, L. (2004). Experimental evaluation of the seismic performance of reinforced concrete bridge columns. *Journal of Structural Engineering* **130:6**, 869-879.

Mazzoni, S., McKenna, F. and H.Scott, M. (2006). OpenSees Command Language Manual. Open System for Earthquake Engineering Simulation (OpenSees).P.Berry, M., Lehman, D. E. and N.Lowes, L. (2008). Lumped-plasticity models for performance simulation of bridge columns. *ACI Structural Journal*, **Vol 105**, 270-279.

P.Berry, M. et O.Eberhard., M. (2007). Performance modeling strategies for modern reinforced concrete bridge columns. *PEER report*. Univesity of California, Berkeley.

Pellegrino, C. And Modena, C. 2010. Analytical Model for FRP confinement of Concrete Columns with and without Internal Steel Reinforcement. *Journal of Composites for Construction.* **14:6**, 693-705.

Samaan, M., Mirmiran, A. and Shahaway, M. (1998). Model of concrete confined by fiber composites. *Journal of Structural Engineering, ASCE*, **124:9**, 1025-1031.

Sause, R., Harries, K. A., Walkup, S. L., Pessiki, S. and Ricles, J. M. (2004). Flexural behavior of concrete columns retrofitted with carbon fiber-reinforced polymer jackets. *ACI Structural Journal*, **101 :5**, 708-716.

Teng, J. G. and Lam, L. (2004). Behavior and modeling of fiber reinforced polymer-confined concrete. *Journal of Structural Engineering, ASCE*, **130:11**, 1713-1723.